Applied Catalysis B: Environmental 84 (2008) 577–583

Contents lists available at ScienceDirect

Applied Catalysis B: Environmental

journal homepage: www.elsevier.com/locate/apcatb

Bacterial inactivation and organic oxidation via immobilized photo-Fenton reagent on structured silica surfaces

Alejandro Moncayo-Lasso [a], Ricardo A. Torres-Palma [b,c], John Kiwi [b], Norberto Benítez [a,**], César Pulgarin [b,*]

[a] Universidad del Valle, Facultad de Ciencias Naturales y Exactas, Departamento de Química, Grupo de Investigación en Procesos de Oxidación Avanzada (GAOX), A. A. 25360, Cali, Colombia
[b] Ecole Polytechnique Fédérale de Lausanne (EPFL), Institute of Chemical Science and Engineering, GGEC, Station 6, CH-1015 Lausanne, Switzerland
[c] Universidad de Antioquia, Facultad de Ciencias Exactas y Naturales, Instituto de Química, Grupo de Electroquímica, A. A. 1226, Medellín, Colombia

ARTICLE INFO

Article history:
Received 28 February 2008
Received in revised form 14 May 2008
Accepted 17 May 2008
Available online 5 June 2008

Keywords:
Photo-catalysis
Heterogeneous photo-Fenton
Advanced oxidation processes
Bacterial inactivation
Organic matter oxidation
Silica fabric

ABSTRACT

A woven inorganic silica fabric loaded with Fe-ions (EGF-Fe) was tested under simulated solar light during hydroquinone degradation. The abatement of hydroquinone was observed to attain about ~80% within 3 h. The photo-catalyst was also tested to inactive *Escherichia coli* K12 at "natural" pH and in the presence of a low concentration of H_2O_2. Addition of H_2O_2 (10 mg L^{-1}) did not by itself to bacterial inactivation. Total bacterial inactivation was mediated by EGF-Fe fabrics in the presence of H_2O_2 (10 mg L^{-1}) under solar light irradiation. A sample containing active (culturable) bacteria (~10^5 CFU mL^{-1}) decreased to values <1 CFU mL^{-1} within 3 h reaction. Fe-mediated homogeneous process decreased the bacterial CFU content by about two orders of magnitude within 4 h. During the degradation of hydroquinone only a small amount of iron ions were found in solution of about 1.2 mg L^{-1}, within 90 min decreasing to values ≤0.5 mg L^{-1} after 180 min. The leaching of Fe-ions did not affect the photo-catalyst performance since EGF-Fe fabric did not deactivate after five or more cycles. The Fe-ions founds in solution mineralized hydroquinone to levels below 37% of its initial content. The present study presents the first report on the beneficial role of a heterogeneous iron supported catalyst leading to efficient bacterial inactivation in aqueous solution with iron leaching <0.1 mg L^{-1}, the detection limit for Fe-analysis in solution. No bacterial re-growth was observed during a post-irradiation period up to 24 h in the dark.

1. Introduction

The most common disinfectant in drinking water treatments is the chlorine leading to chloro-organic compounds when it is in contact with dissolved organic matter. These are carcinogenic and mutagenic chloro-organic compounds commonly known as disinfection by-products (DBPs) [1]. In order to minimize the health risk to humans, modifications of this with concomitant removal of chloro-organic compounds, have been proposed [2,3].

In recent years solar radiation, for bacterial disinfection and the degradation of organic matter in aqueous solution have been explored [4–6]. It is a useful approach for regions with a high degree of sunlight radiation. The photo-Fenton system seems an effective option for the treatment of wastewaters as well as for water disinfection [2,7–8].

Fenton's reagent action is based on the reaction of H_2O_2 with Fe(II)/Fe(III) ions, producing $^{\bullet}OH$ radicals and other highly oxidative species in solution. The homogeneous Fenton (Eq. (1)) and photo-Fenton processes (Eqs. (1) and (2)) are used in the treatment of organics pollutants [9,10] and more recently for bacterial inactivation. The overall process is described in Ref. [11,12–17].

$$Fe^{2+} + H_2O_2 \rightarrow Fe^{3+} + HO^- + {}^{\bullet}OH \quad (1)$$

$$Fe(OH)^{2+} + h\nu \rightarrow Fe^{2+} + {}^{\bullet}OH + H^+ \quad (2)$$

The effect of the light irradiation is seen in Eq. (2) regenerating (Fe^{2+}) by photo-reduction of the aqua-Fe(III) complexes leading to the additional production of $^{\bullet}OH$ radicals. The main advantage of the photo-Fenton process is the light absorption up to 600 nm comprising 35% of the solar spectrum. Additionally, in homogeneous photo-Fenton process, the interaction between pollutant and

* Corresponding author. Tel.: +41 21 693 47 20; fax: +41 21 693 56 90.
** Corresponding author. Tel.: +57 2 3393248; fax: +57 2 3392440.
E-mail addresses: lubenite@univalle.edu.co (N. Benítez), cesar.pulgarin@epfl.ch (C. Pulgarin).

0926-3373/$ – see front matter © 2008 Elsevier B.V. All rights reserved.
doi:10.1016/j.apcatb.2008.05.022

oxidizing agent is favored [12]. But the use of the Fenton's reagent as homogeneous catalyst implies several drawbacks. Only a limited range of pH (2.5–4.0) is useful due to the range of solubility of Fe-ions, otherwise $Fe(OH)_3$ settles beginning at pH 4.0 and the reaction takes place with very low efficiency. Homogeneous Fenton treatment, implies to recovery of Fe-ions to comply with environmental regulations related to water standards. Therefore the necessity for the design, synthesis and testing of Fe-supported photo-catalysts effective in pollutant degradation and bacterial disinfection is warranted. Hereby, we report the immobilization of photoactive iron-species on inorganic fabrics useful at higher pH-values than the range available to the homogeneous system.

Previous studies on supported Fe-ions photo-catalysts have involved perfluorinated membranes [18], Nafion-silica composites [19], polyethylene copolymers [20], Fe/C structured fabric [21–23], etc. However, the first three materials were high cost and showed low photo-catalytic activity. When the Fe/C structured fabric was used a high hydrogen peroxide concentration was needed. Ferric species has been also immobilized on ionic exchange resins [24], composite of iron oxide and silicate nano-particles [25] and amorphous, zeolitic and meso-structured materials [26]. Other materials containing crystalline hematite particles embedded into meso-structured SBA-15 matrix [27], Fe(III)-HY zeolites [28], saponite [29] or montmorillonite clays [30] have shown to effectively degrade pollutants with a low Fe-leaching rate. However, a pH 3.0 was required for some catalyst to obtain high degradation percentages. At higher pH values the mineralization percentages decreased markedly specially at pH-values 5.5–6.5 usually required for drinking water.

The suitable properties of a support like the EGF fabric for Fe-ions immobilization are: (a) to be resistant towards the highly oxidative radicals formed in solution, (b) to allow a very low leaching of Fe-ions from the support during reactor operation, (c) to intervene with adequate kinetics in the degradation process and (d) the support should enable long-term stability during reactor operation [31].

Woven fibrous glass fabrics have become interesting supports for reactor processes because they present an open microstructure. They possess adequate mechanical and thermal resistance since the catalyst preparation required several hundred degrees [32,33]. Silica fabrics have been recently reported useful in oxalic acid degradation, showing adequate stability and low Fe-ions leaching [34].

The present work uses EGF-Fe fabrics prepared by a procedure recently reported [34–36] to mediate hydroquinone degradation and the bacterial inactivation of *Escherichia coli* (*E. coli*). Hydroquinone is a model compound found in natural waters producing during the degradation of organic matter, while that *E. coli* is the most popular indicator of biological contamination.

2. Experimental

2.1. Reagents

Acetonitrile, acetic acid, potassium phthalate, hydroquinone, benzoquinone, HCl, HF, ferric chloride hexahydrated, ferrous sulfate, ferrizine, sodium bisulphite and potassium thiocyanate were obtained from Fluka (Buchs, Switzerland) and used as received. Hydrogen peroxide was supplied by Merck AG (Darmstadt, Germany). All solutions were prepared with Millipore water (18.2 MV cm at 25 °C) and used immediately prior to irradiation.

2.2. Preparation and characterization of supported Fe/silica fabrics (EGF-Fe)

The alumino-borosilicate fibers from Vetrotex were treated with HCl to leach out all the non-silica components (SiO_2, B_2O_3, MgO, Al_2O_3, K_2O, Na_2O) [35,36]. The ion-exchange of Fe-ions on the silica fibers was carried out in a batch type operation with ferrous sulfate (5×10^{-2} M) at room temperature. The fabrics were dried at room temperature and calcined at 450 °C for 1 h. The samples were rinsed with distilled water and dried in air at room temperature [34,36]. The loading of 0.4% Fe by weight of the silica fibers was determined dissolving the loaded iron in a mixture of HCl (37%): HNO_3 (65%) = 1:4, with 1 mL L^{-1} of HF added in solution. The Fe-ions were determined subsequently spectrophotometrically with the ferrizine reagent.

The EGF-Fe fabrics were characterized by infrared spectroscopy (ATRIR), transmission electron microscopy (TEM), energy dispersive X-ray spectrometry (EDS) and X-ray photoelectron spectroscopy (XPS). Attenuated total reflection infrared spectroscopy (ATRIR) was applied to the study of Fe-silica structured surfaces. The reflection spectra were recorded on a Bruker IFS 55 FTIR spectrophotometer equipped with a calcium telluride detector and an internal reflection attachment from Harrick Co. The ATRIR technique was recently reported [38].

Electron microscopy (TEM) observations were performed on a Philips CM 300UT/FEG microscope fitted with a Schottky field emission gun operated at 300 kV and using an objective lens with a very short spherical aberration coefficient (0.65 nm). Semi-quantitative chemical analysis was performed using an EDS of Oxford Inc., UK with an organic detector window. To monitor the sample composition, probes having 10 μm diameter were tested

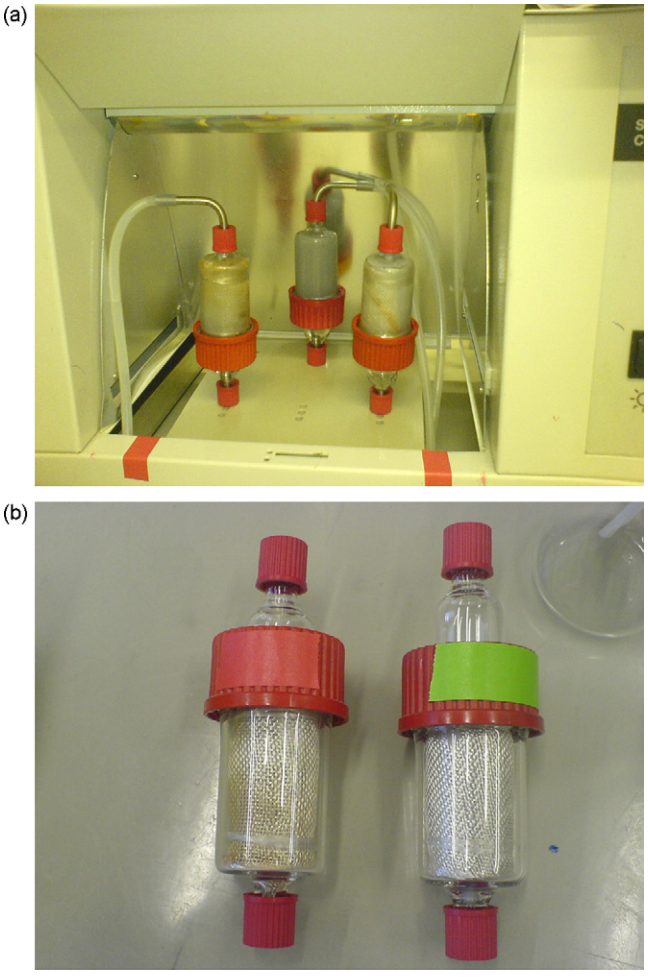

Fig. 1. (a) Thin film reactors in solar lamp. (b) Thin film reactor with EGF-Fe loaded on an internal PVC support. Fabric area (70 cm^2), iron loaded/area fabric relation = 0.08 mg Fe cm^{-2}.

on weakly irradiated samples. The ring patterns superimposed on an intense background showed a contrast that was sufficient for accurate phase determination.

The XPS experiments were performed with a Leybold-Heraeus instrument (LHS 12) using Mg Kα radiation set at 200 W of power. The binding energies of the peaks were referenced to the Au $4f_{7/2}$ energy level of 84 eV. The spectra were analyzed in a DS-100 dataset (Leybold) after X-ray satellite subtraction and smoothing by polynomial fit. The quantitative evaluation of the background correction used the standard Shirley treatment [39]. The relative sensitive factors found were: Fe 2p: 2.91, O 1s: 0.78, C 1s: 0.34, S 2p: 0.84. Electrostatic charging effects were referenced to the C 1s signal. Charge compensation measurements involved changing the electrostatic potential at the entrance slit of the XPS-electron analyzer.

2.3. Photo-reactors and light sources

All experiments were carried out using thin film Pyrex glass reactors with an illuminated volume of 25 mL (Fig. 1a). A peristaltic pump recirculated the water with a flow rate of 150 mL min^{-1}. The total volume of the system (110 mL) can be distinguished in two parts: 25 mL of irradiated volume and the dead volume (recirculation tank + connecting tubing). Internal PVC supports were put in the reactors to carry the EGF-Fe fabric (70 cm^2) (Fig. 1b). The reactor was illuminated from outside with a solar lamp CPS Suntest system (Atlas GmbH) with a spectral distribution of 0.5% of the photons <300 nm, and about 7% between 300 and 400 nm. The emission spectrum between 400 and 800 nm follows the solar spectrum. The irradiation experiments (750 W m^{-2}) were started at room temperature (25 °C) and the temperature increased up to approximately 32 °C during irradiation. The solutions pH was not modified. For hydroquinone degradation, the initial pH was of 5.0 and for bacterial inactivation it was of 6.0. Suitable dark control experiments were performed under similar conditions. Six reactors could be placed in parallel inside the reactor lamp cavity.

2.4. Analysis of the irradiated solutions

The determination of hydroquinone was carried out by HPLC chromatography in a Waters Associates 590 instrument with a Nucleosil C-18 column (i.d. = 4.6 mm, length = 250 mm) and a UV detector set at 280 nm. The mobil phase consisted of an acetonitrile–acetic acid solution (1%) in a 30–70% and was run in isocratic mode (1 mL min^{-1}). The total organic carbon (TOC) was monitored in a Shimadzu 500 equipped with an ASI automatic sample injector. The peroxide concentrations were assessed by Merkoquant paper® at levels between 0.5 and 25 mg L^{-1}. The samples were measured immediately after taking the sample out of the reactor and when the samples were not immediately analyzed, the reaction was stopped with sodium bisulphite. The total iron concentration in the irradiated solutions was measured by complexation with Ferro-zine® (Aldrich 16.060-1) in the presence of hydroxylamine hydrochloride.

2.5. Bacterial strain and growth media

A complete description was presented previously [40]. The bacterial strain used, *E. coli* K12 (ATCC 23716), was supplied by DSM (German Collection of Microorganisms and Cell Cultures). *E. coli* K12 was inoculated into Luria Bertani (LB) medium and grown overnight at 37 °C by constant agitation under aerobic conditions. Components of LB medium included sodium chloride (10 g), tryptone (10 g) and yeast extract (5 g) in 1 L of de-ionized water; this solution was then sterilized by autoclaving for 20 min at 121 °C. Aliquots of the overnight grown culture were inoculated into sterilized LB medium and incubated aerobically at 37 °C. The bacterial cells were collected in a stationary phase, by centrifugation at 5000 rpm for 10 min at 4 °C, and the bacterial pellet was washed three times with a tryptone solution (1%, w/v). Finally, the bacterial pellet was re-suspended in tryptone solution and diluted in de-ionized water to the required cell density corresponding to 10^4–10^5 colony forming units per milliliter (CFU mL^{-1}). Thereafter, bacterial suspension was exposed to the sunlight irradiation in the presence of EGF-Fe fabric. Illuminated samples were taken during illumination period (4 h) and after 24 h in the subsequent dark period. Samples were plated on agar Plate—Count-Agar (PCA, Merck, Germany) plates, samples were not filtered prior to plating. Colonies were enumerated after 24 h incubation at 37 °C. The error

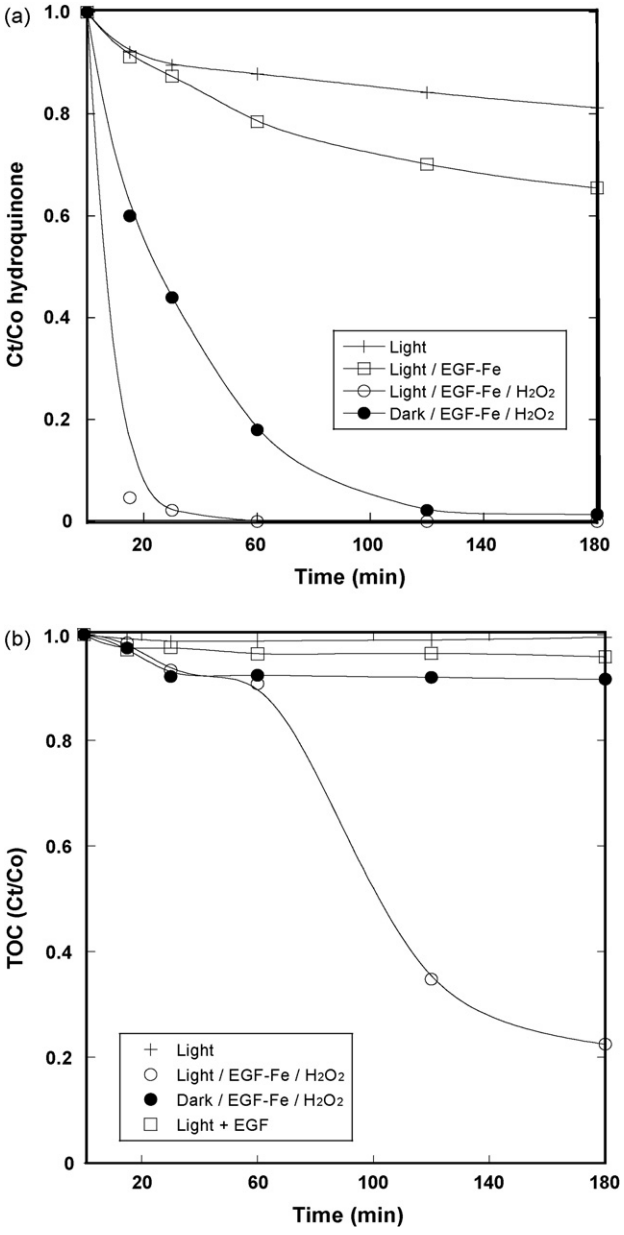

Fig. 2. Degradation (a) and mineralization (b) of hydroquinone (20 mg L^{-1}) at natural pH (5.8) under Suntest light irradiation (750 W m^{-2}) in a solution containing H_2O_2 (40 mg L^{-1}) using EGF-Fe fabric. These dates correspond to the fifth cycling.

bars indicate the standard deviation (S.D.) found during the determination of these samples.

In order to test dark repair experiments at predetermined exposure times, the samples were removed from the photo-reactor and wrapped with aluminum foil immediately after light exposure. Duplicate samples were transferred to an incubator under mechanical agitation at 37 °C for 24 h. The duplicate samples were plated for counting after 24 h incubation.

3. Results and discussion

3.1. Study of hydroquinone degradation

3.1.1. Evaluation of EGF-Fe photo-catalytic activity

Fig. 2 shows the hydroquinone evolution (Fig. 2a) and mineralization (Fig. 2b) as a function of the irradiation time under different conditions. Applying only light, after 3 h of treatment, the hydroquinone concentration decreases (10–15%) while the mineralization degree is insignificant (Fig. 2b trace -+-). Under light irradiation and in the presence of the EGF-Fe fabric a clear increment in both, hydroquinone degradation (30%) (Fig. 2a trace -□-) and mineralization (4%) was observed. This effect probably involves charge transfer between hydroquinone and surface Fe(III) ions, complex formation and due to the low amount of Fe(III) ions leached in solution from photo-dissociation of iron oxides present on the EGF-Fe fabric [34,41,42]. A faster degradation and mineralization rate was achieved in presence of H_2O_2 under Suntest irradiation in the presence of the EGF-Fe fabric (Fig. 2, trace -○-) leading to hydroquinone disappearance (Fig. 2a), and to a 80% mineralization (Fig. 2b) within 1 and 3 h treatment respectively. In the absence of light but in presence of H_2O_2 and EGF-Fe (dark Fenton reaction) the hydroquinone was degraded in 3 h (Fig. 2a, trace -●-); whereas during the same time, the TOC removal is lower than 10% (Fig. 2b, trace -●-). In a control experiment, the hydroquinone adsorption on the EGF-Fe fabric was observed to be almost negligible. The H_2O_2 concentration after 3 h of treatment was <0.5 mg L^{-1}. These results show the efficiency of the EGF-Fe/H_2O_2/light system to degrade hydroquinone.

3.1.2. Stability of the EGF-Fe fabric in the heterogeneous photo-Fenton degradation of hydroquinone

Successive hydroquinone degradation cycles mediated by the EGF-Fe fabric were carried out (Fig. 3). After each run, the EGF-Fe was thoroughly washed with distilled water. Then, a new solution of hydroquinone and H_2O_2 was added before the next cycle. No deactivation of the fabric was observed when compared with the first cycle and a mineralization percentage ~80% was attained in each cycle within 3 h.

3.1.3. Leaching of iron species from EGF-Fe during photo-catalytic process

An important point in the design of heterogeneous catalytic systems for advanced oxidation processes is the sticking of the Fe-from onto the aqueous solution in oxidative media.

Fig. 4 shows the evolution of iron concentration in solution during photo-catalytic processes similar to the values reported in Fig. 3 for hydroquinone degradation. It was found that the concentration of Fe-ion increased during the first half hour of reaction to 1.2 mg L^{-1} and then decreased reaching values ≤ 0.5 mg L^{-1}. This observation has been also reported for other Fe(III) immobilized photo-catalysts [34,43–44].

Some authors have associated this Fe-leaching with the generation of Fe-complexes with organic oxidation by-products of the hydroquinone degradation like, i.e. oxalic acid that detach iron ions from the fabric [45]. Thereafter, when organic ligands are degraded, the Fe-ions can return to the surface of the catalyst since by inertia the surface of EGF-Fe is the predominating containing Fe-material and would be able to incorporate easily the Fe-ions into the Fe_2O_3 present on the catalyst surface. From the Figs. 2b and 4, after ca. 60 min, the mineralization rate increases and the Fe concentration in solution decreases.

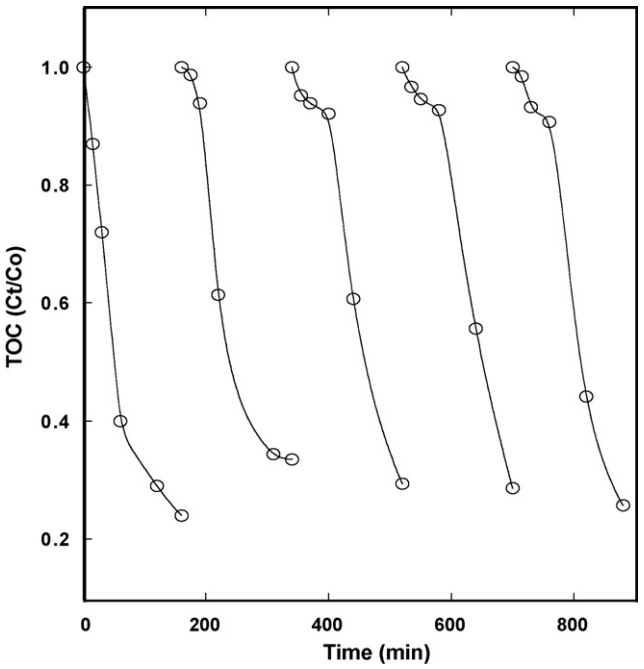

Fig. 3. Repetitive catalytic mineralization cycles of hydroquinone (20 mg L^{-1}), natural pH (5.8); under Suntest light irradiation (750 W m^{-2}) in presence of EGF-Fe and H_2O_2 (40 mg L^{-1}).

Fe-oxy-hydroxy (–Fe–O–Fe–) (active catalytic iron species) and Fe-silicate (–Si–O–Fe–) were species found by IR Peaks at 1635 cm^{-1} corresponding to the Fe-oxy-hydroxy band [46,47]. Numerous studies have shown that Fe(III)-hydrous- oxides undergo photo-reduction reactions. These reactions are an

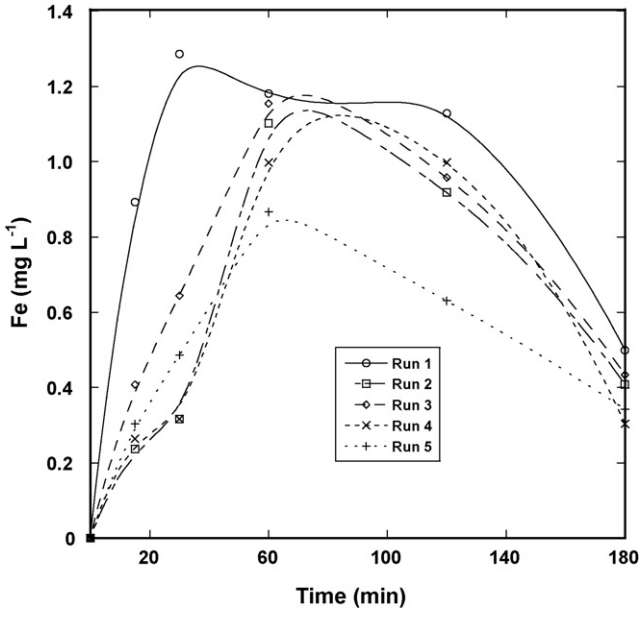

Fig. 4. Fe-ions concentration as function of the reaction time within five degradation cycles.

important pathway for dissolving solids Fe(III)-oxides [48]. Indeed, when the surface metal species are in the lower valence form, the charge to radius ratios is smaller. This leads to a weakening of the metal–oxygen bonds in the Fe-oxide lattice [36] that can be easier attacked by H_2O_2. The mechanism is complex, however in a first step, Fe(III) is reduced to Fe (II) through of photo-redox reactions

$$\equiv Fe(III)_{Amorphous} + h\nu \rightarrow \equiv Fe(II) \quad (3)$$

In the second stage, Fe (II) can react with H_2O_2 to produce $^{\bullet}OH$ in solution [49]

$$\equiv Fe(II) + oxidant(H_2O_2) \rightarrow [Fe(III)_{Dissolved}/\equiv Fe(III)] + OH^- + HO^{\bullet} \quad (4)$$

Latter, Fe(III) can be subsequently re-adsorbed

$$Fe(III)_{Dissolved} \rightarrow \equiv Fe(III) \quad (5)$$

The Fe(III) is more likely to form amorphous precipitates, which have a much higher solubility than crystalline Fe(III)-hydrous-oxides. Thus, photo-redox reactions may lead to dissolved iron through photo-dissolution reactions and through the formation of amorphous Fe(III)-species with a higher solubility than crystalline Fe.

In order to evaluate the contribution of leached Fe photoactive species to the hydroquinone mineralization, two homogeneous photo-Fenton experiments were carried out. In the first experiment $FeCl_3{\cdot}6H_2O$ was used as the source of iron. A Fe-concentration of 1 mg L^{-1} of Fe(III) was chosen because the leaching of iron species during photo-degradation runs was around this value (Fig. 4). When Fe^{3+} (1 mg L^{-1}) and H_2O_2 (40 mg L^{-1}) were added to the solution containing hydroquinone, 2 h were necessary to fully degrade hydroquinone. Moreover, 30% of mineralization was reached within 3 h (Fig. 5, trace –◇–). In the second control experiment, at the end of a hydroquinone degradation cycle, the EGF-Fe fabric was removed of the system and both hydroquinone (20 mg L^{-1}) and hydrogen peroxide (40 mg L^{-1}), were added again to the original solution. Fig. 5 (trace –△–) shows a TOC removal similar the one obtained by addition of Fe^{3+} ions in solution. The results show that 80% of mineralization with the EGF-Fe fabric (Fig. 5, trace –○–) was reached within 3 h in a dual process involving heterogeneous–homogeneous photo-catalysis. The contribution of leached Fe photoactive species to the hydroquinone mineralization was around 37%.

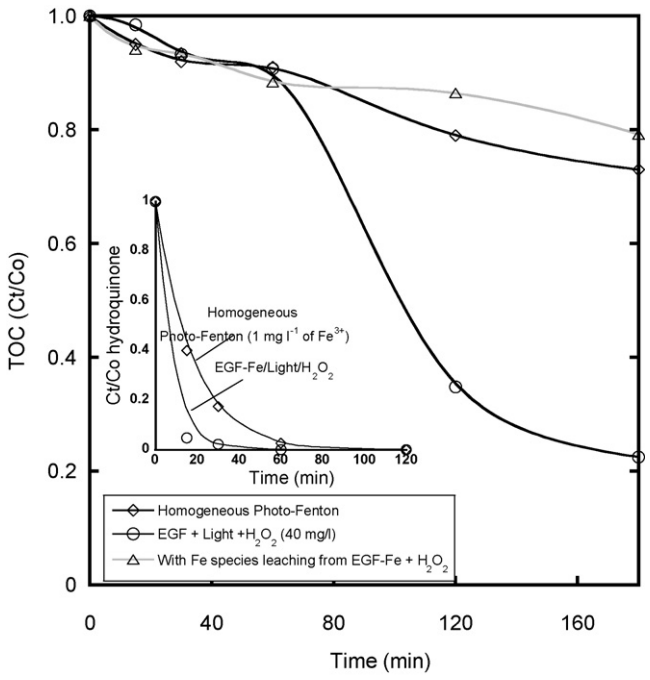

Fig. 5. TOC evolution of hydroquinone degradation via: homogeneous photo-Fenton (trace –◇–) adding $FeCl_3{\cdot}6H_20$ (1 mg L^{-1}) and with Fe species leached from EGF-Fe (trace –△–). Initial pH for homogeneous photo-Fenton 4.3–4.8. And heterogeneous photo-Fenton using EGF-Fe under Suntest light irradiation (750 W m^{-2}) and H_2O_2 (40 mg L^{-1}). Initial pH for heterogeneous photo-Fenton 5.5–5.8. Hydroquinone concentration (20 mg L^{-1}). Insert graph: evolution of hydroquinone concentration.

3.2. Bacterial inactivation

It has been already reported that the homogeneous photo-Fenton process led to bacterial inactivation close to pH 6.5 and in the presence of a low concentration hydrogen peroxide and Fe^{3+} ions [17]. In Fig. 6 the bacterial cultivability is plotted against time for dark runs, light runs, in the absence or presence of H_2O_2 and in absence or presence of the EGF-Fe. The experiments were carried out with bacteria in stationary phase of culturability. The initial pH of the solutions was 6.5 and decreased to 5.5 during the reaction for solutions with 10 mg L^{-1} of H_2O_2.

3.2.1. Light alone

Fig. 6 show that the reduction of *E-coli* in de-ionized water (trace -X-) was about one order of magnitude within 4 h of treatment. These results are in agreement with those reported by Gumy et al. [50] in the same reactor using the same initial bacteria concentration. The poor inactivation observed only due to the effect of light can be explained because the stationary-phase response to environmental changes involves the synthesis of a set of proteins, which confer *E. coli* cells a marked resistance to stress conditions, including heat shock, UV light, hyperosmolarity, acidity, and nutrient scarcity [51–52].

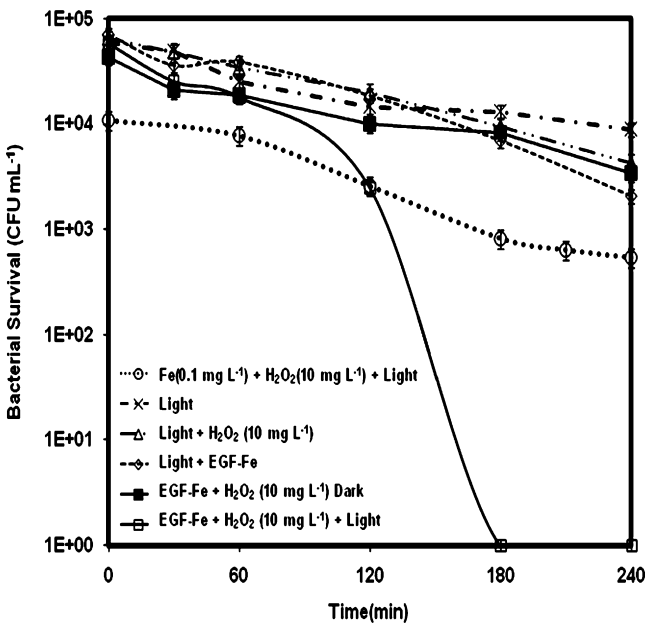

Fig. 6. *E. coli* inactivation under simulated solar illumination in the presence and absence of EGF-Fe. Light/EGF-Fe/H_2O_2 system (-□-), H_2O_2/Light (-△-), light alone (-x-). Dark control represents bacteria/EGF-Fe (-+-), homogeneous photo-Fenton (-○-): Fe^{3+} (0.1 mg L^{-1})/H_2O_2 (10 mg L^{-1}) and Fenton process bacteria/EGF-Fe/H_2O_2 (- * -) H_2O_2 (10 mg L^{-1}); natural pH 6.5–7.0.

3.2.2. Light/H_2O_2 system

Fig. 6 (trace -△-) shows that during the *E. coli* inactivation by UV–vis light in the presence of 10 mg L^{-1} (0.3 mmol L^{-1}) H_2O_2. The inactivation kinetics is increased compared to the case when H_2O_2 was absent (trace -x-). It has been demonstrated that H_2O_2 has a direct oxidative action on bacteria rendering them weaker and more sensitive to the photolytic action and, vice versa, the light makes bacteria weaker and more sensitive to H_2O_2. Moreover, the Photo-Fenton reaction inside the cell is probably favored by the addition of H_2O_2 due to the presence of free iron inside the cell. In the re-growing experiments (24 h in dark), the bacterial concentration continues to decrease reaching levels <1 CFU mL^{-1}. The H_2O_2 concentration after 24 h re-growing was <0.5 mg L^{-1}. The results obtained in the dark suggest that this delayed effect depends on the possible presence of residual iron traces in the set-up, light intensity used, and the initial bacteria concentration [53]. The repair mechanism *E. coli* in the dark probably does not take place [40].

3.2.3. Light/EGF-Fe system

Direct germicidal action of light in the presence of EGF-Fe (Fig. 6, trace –◇–) is slightly more efficient than the action of UV–vis light alone. In the absence of H_2O_2, it seems that Fe (<0.1 mg L^{-1}) leaching from the EGF-Fe fabrics may play a role through of mechanism previously suggested. At pH slightly acid, there are four different Fe(III) ions, which coexist at low concentrations in aqueous solution: Fe^{3+}, $Fe(OH)^{+}$, $Fe(OH)^{2+}$ and the dimmer $Fe_2(OH)_2^{4+}$ [33] leading $^{\bullet}OH$ radicals and other highly oxidative radicals with light <580 nm [34–37,40–42] enhance water disinfection [11,35–36,40] compared with solutions where Fe(III) was absent.

The trace amounts of "free iron" into the cell can enhances the intracellular Fenton and photo-Fenton reactions catalyzing the production of $^{\bullet}OH$ via Fenton/Habber–Weiss reaction cycle [48]. Intracellular Fenton and photo-Fenton electron acceptors involve super-oxide anion radical ($O_2^{\bullet-}$) and hydrogen peroxide (H_2O_2) generation during the respiration and bacterial oxidation of carbon nutrients [51,54].

3.2.4. EGF-Fe/H_2O_2 in absence of light

Fig. 6 (trace -⋆-) shows that, during the *E. coli* inactivation by EGF-Fe in the presence of 10 mg L^{-1} (0.3 mmol L^{-1}) of H_2O_2 in the dark, the system was able to inactivate *E. coli*; total disinfection was not reached. The decreased of culturability obtained, of one order of magnitude within 4 h was similar to the results observed when using EGF-Fe fabric under light or in solutions under light with added H_2O_2. Due to low amount of H_2O_2 and Fe^{3+} from EGF-Fe fabric, efficiency of the process is not high.

3.2.5. EGF-Fe/H_2O_2/light system

Fig. 6 (trace -□-) shows that the bacterial inactivation is strongly enhanced in presence of the EGF-Fe/H_2O_2/light. In this case, the number of active (culturable) bacteria decreases to non-detectable values (<1 CFU mL^{-1}) within 3 h of treatment. The photo-catalytic inactivation is mainly due to the attack of oxidative species (i.e. $HO_2^{\bullet}$ and $^{\bullet}OH$) generated on the surface of the supported photo-catalyst. When the bacteria are in contact with the reactive species on surface of the fabric, the cell membrane is attacked, especially by $^{\bullet}OH$, leading to lipid peroxidation and the death of cell. In this system, the production of $^{\bullet}OH$ radicals is probably high due to the high amount of Fe in the fabric. No re-growth of bacteria was observed in the dark after 24 h suggesting a strong bactericide effect taking place. Effective disinfection time (EDT24), which is the required time to reach total inactivation of bacteria without re-growth within a dark period of 24 h, was reached after 3 h irradiation corresponding to an equivalent dose of 2250 W m^{-2} h^{-1} [55].

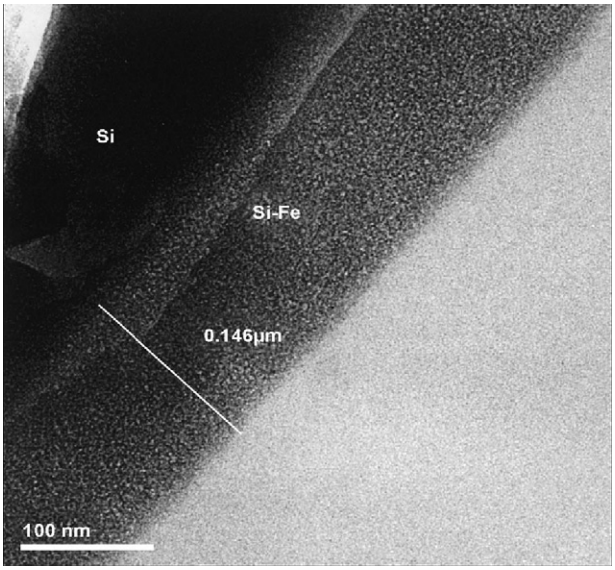

Fig. 7. Transmission electron microscopy (TEM) of the silica fabric showing the interfacial Fe-silicate identified by means of electron dispersive X-ray spectrometry (EDS).

3.2.6. Contribution of homogeneous photo-Fenton in bacterial inactivation

In order to evaluate the contribution of leached Fe during bacterial inactivation, the total Fe-concentration in solution was quantified and was found to be below the detection limit of 0.1 mg L^{-1}. Homogeneous photo-Fenton runs (Fe^{3+}, 0.1 mg L^{-1} / H_2O_2, 10 mg L^{-1}) was carried out in order to assess the relative contribution of the leached Fe species on CFU concentration in solution. Under these conditions, total disinfection was not reached. A culturability decrease of around two orders of magnitude after 4 h of treatment was observed (Fig. 6, trace (-○-)). These results show that the inactivation due to the homogeneous process is not important compared to the heterogeneous processes going on in solution mediated by EGF-Fe fabrics.

No bacterial detection was possible after re-growth due to Fenton processes in the dark proceeding with lower inactivation kinetics compared to photo-Fenton processes.

3.3. Characterization of EGF-Fe by transmission electron microscopy and XPS of the EGF-Fe fabrics

Fig. 7 obtained by HRTEM shows Fe-clusters with sizes ≤1 nm homogeneously distributed on the silica fabric. EDS of these samples shows the presence of –Si–O–Fe– species in the EGF-fabric. A layer of 0.146 μm thick is observed.

Table 1
Elemental analysis by XPS of silica and EGF/Fe fabrics

Element peak	EGF-Fe fabric	Silica fabric
C 1s	12.7	26
N 1s	0.43	0.77
O 1s	51.3	43
F 1s	2.25	0.75
Si 2p	22.6	27.5
Ca 2p	3.29	0.47
Fe 2p	5.06	<0.1

Table 2
Binding energies of the Fe ion in EGF/Fe fabric

Spectral peak	Before use		After use	
	BE (eV)	%	BE (eV)	%
Fe $2p_{3/2}$	708.9	0.01	708.8	0.03
Fe $2p_{3/2}$ ox	711.2	59.6	710.9	57.8
Fe $2p_{3/2}$ ox'	713.4	40.4	713.0	42.2

XPS spectroscopy determined the elements on the silica surface and was carried out according to DIN [56] comparing with known spectra of silica. Carbon was removed during the preparation of the Fe-loaded silica fabric decreasing from 26 to 12.7% during the preparation (see Table 1). Other species as surface fluorine were seen to increase (from 0.75 to 2.25%) due to the migration of the F during the calcination step. The Fe present covers more than 5% of the fabric, which is a surprisingly high value compared with the percentage on silica fiber without loaded-Fe (<0.1). The small cluster size and the high surface coverage seem to be the factors responsible for the high catalytic activity observed with the EGF-Fe fabric. The binding energy (BE) of the Fe_{2p} doublet was seen to shift slightly after photo-catalysis for the EGF-Fe fabric (Table 2). This is indicative of a small reduction of Fe(III) (peak at 711.2 eV) to Fe(II) (peak at 708.9 eV) after the EGF-Fe fabric has been used as a photo-catalyst in some runs. This is confirmed by the fading of the initial pale orange color observed to yellow color for the fabrics after use since FeO/Fe(II) is colorless. Other peak observed at 713.4 eV originates from the peak asymmetry observed in the Fe-oxide band envelope (FeO/Fe_2O_3).

4. Conclusion

This work demonstrates that photo-Fenton process with EGF-Fe fabric is a suitable heterogeneous catalyst to abate pollutants and bacterial at a pH close to neutral, in the presence of a low concentration of H_2O_2 and with a low amount of iron leached in solution. The EGF-Fe fabric shows good-term stability, since upon reuse no deactivation of the fabric was observed. The EGF-Fe fabric seems to be a suitable heterogeneous system for bacterial inactivation not allowing bacterial re-growth in the dark up to 24 h.

Acknowledgements

Very thanks to Julian Rengifo for his scientific and technical help. We gratefully acknowledge to COLCIENCIAS-Colombia for scholarship granted to Alejandro Moncayo. Our special thanks to UNIVALLE-EPFL cooperation program supported by the Cooperation@EPFL and to EPFL and Swiss Agency for Development and Cooperation for its support to Biosolar-Detox project.

References

[1] R.J. Bull, F.C. Kopfler, Health Effects of Disinfectants and Disinfection Byproducts, American Water Works Association Research Foundation, Denver, CO, 1991.
[2] W.J. Cooper, E. Cadavid, M.G. Nickelsen, K.J. Lin, C.N. Kurucz, T.D. Waite, J. Am. Water Work Assoc. 85 (1993) 106.
[3] D.W. Hand, D.L. Perram, J.C. Crittenden, J. Am. Water Work Assoc. 87 (1995) 84.
[4] D. Bahnemann, J. Cunningham, M.A. Fox, E. Pelizzetti, P. Pichat, N. Serpone, in: G.R. Helz, R.G. Zepp, D.G. Crosby (Eds.), Aquatic and Surface Photochemistry, Lewis Publishers, Boca Raton, 1994, pp. 261–316.
[5] C. Pulgarin, J. Kiwi, Chimia 50 (1996) 50–55.
[6] P. Ribordy, C. Pulgarin, J. Kiwi, P. Peringer, Water Sci. Technol. 35 (1997) 293–302.
[7] A.G. Rincon, C. Pulgarin, J. Sol. Energy Eng. 129 (2007) 100–110.
[8] J. Bandara, C. Pulgarin, P. Peringer, J. Kiwi, J. Photochem. Photobiol. A 111 (1997) 253–263.
[9] M.R. Hoffmann, S.T. Martin, W.Y. Choi, D.W. Bahnemann, Chem. Rev. 95 (1995) 69.
[10] J. Hoigne, Water Sci. Technol. 35 (1997) 1.
[11] A. Rincón, C. Pulgarin, Appl. Catal. B 63 (2006) 222–231.
[12] R. Bauer, G. Waldner, H. Fallmann, S. Hager, M. Klare, T. Krutzler, S. Malato, P. Maletzky, Catal. Today 53 (1999) 131.
[13] H. Fallmann, T. Krutzler, R. Bauer, S. Malato, J. Blanco, Catal. Today 54 (1999) 309.
[14] F. Herrera, C. Pulgarin, V. Nadtochenko, J. Kiwi, Appl. Catal. B 17 (1998) 141.
[15] J. Kiwi, C. Pulgarin, P. Peringer, Appl. Catal. B 3 (1994) 335.
[16] M. Rodriguez, V. Timokhin, F. Michel, S. Contreras, J. Gimenez, S. Esplugas, Catal. Today 76 (2002) 291.
[17] A. Rincón, C. Pulgarin, Catal. Today 122 (2007) 128–136.
[18] J. Fernandez, J. Bandara, A. Lopez, P. Buffat, J. Kiwi, Langmuir 15 (1999) 185–193.
[19] M. Dhananjeyan, J. Kiwi, P. Albers, O. Enea, Helv. Chim. Acta 84 (2001) 3433–3441.
[20] M. Dhananjeyan, E. Mielczarski, R. Thampi, P. Buffat, M. Bensimon, A. Kulik, J. Mielczarski, J. Kiwi, J. Phys. Chem. 105 (2000) 12046–12053.
[21] A. Bozzi, T. Yuranova, P. Lais, J. Kiwi, Water Res. 39 (2005) 1441–1450.
[22] T. Yuranova, O. Enea, E. Mielczarski, J. Mielczarski, P. Albers, J. Kiwi, Appl. Catal. B. 49 (2004) 39–50.
[23] D. Gumy, P. Fernandez-Ibanez, S. Malato, C. Pulgarin, O. Enea, J. Kiwi, Catal. Today 101 (2005) 375–382.
[24] X. Lv, Y. Xu, K. Lv, G. Zhang, J. Photochem. Photobiol. A 173 (2005) 121–127.
[25] J. Feng, X. Hu, P.L. Yue, Ind. Eng. Chem. Res. 42 (2003) 2058–2066.
[26] F. Martínez, G. Calleja, J.A. Melero, R. Molina, Appl. Catal. B 70 (2007) 452–460.
[27] F. Martínez, G. Calleja, J.A. Melero, R. Molina, Appl. Catal. B 60 (2005) 181–190.
[28] M. Noorjahan, V. Durga-Kurami, M. Subrahmanyam, L. Panda, Appl. Catal. B 57 (2005) 291–298.
[29] J. Ramirez, C. Costa, L. Madeira, G. Mata, M. Vicente, M. Rojas-Cervantes, A. Lopez-Peinado, R. Martin-Aranda, Appl. Catal. B 71 (2007) 44–56.
[30] W. Song, M. Cheng, J. Ma, W. Ma, C. Chen, J. Zhao, Environ. Sci. Technol. 40 (2006) 4782–4787.
[31] R. Bauer, G. Waldner, S. Hager, S. Malato, P. Maletzky, Catal. Today 53 (1999) 131–144.
[32] L. Kiwi-Minsker, I. Youranov, B. Siebenhaar, A. Renken, Catal. Today 54 (1999) 39–45.
[33] V. Höller, K. Radevic, I. Youranov, L. Kiwi-Minsker, A. Renken, Appl. Catal. B 32 (2001) 143–150.
[34] A. Bozzi, T. Yuranova, J. Mielczarski, J. Kiwi, New. J. Chem. 28 (2004) 519–526.
[35] L. Kiwi-Minsker, J. Yuranov, E. Slavinskaia, V. Zaikovski, A. Renken, Catal. Today 59 (2000) 61.
[36] A. Bozzi, T. Yuranova, J. Mielczarski, E. Mielczarski, P.A. Buffat, J. Kiwi, Appl. Catal. B 42 (2003) 289–303.
[37] R. Hoffmann, Angew. Chem. 99 (1987) 871.
[38] N.J. Harrick, Internal Reflection Spectroscopy., Harrick Scientific Ossinning, New York, 1987.
[39] A. Shirley, Phys. Rev. 135 (1979) 4709.
[40] A.G. Rincón, C. Pulgarin, Appl. Catal. B 49 (2004) 99–112.
[41] N. Yoshida, T. Matsuchita, S. Saigo, H. Oyanagi, H. Hashimoto, M. Fujimoto, J. Chem. Soc. Chem. Commun. (1990) 354–356.
[42] D.M. Sherman, Geochim. Cosmochim. Acta 69 (2005) 3249–3255.
[43] R. Tang, X.P. Liao, X. Liu, B. Shi, Chem. Commun. (2005) 5882-L5884.
[44] J. Fenga, X. Hua, P.L. Yue, H.Y. Zhub, G.Q. Lu, Chem. Eng. Sci. 58 (2003) 679–685.
[45] J. Feng, X. Hu, P.L. Yue, Water Res. 40 (2006) 641–646.
[46] R.C. Mehrotra, R. Bohra, Metal Carboxylates, Academic Press, London, 1983.
[47] M. Edward, C. Russell, J. Mol. Struct. 443 (1998) 223–229.
[48] G.R. Heltz, R.G. Zepp, D.G. Crosby, Aquatic and Surface Photochemistry, Lewis Publishers, 1994.
[49] M. Sulzberger, R. Laubscher, R. Marine, Mar. Chem. 50 (1995) 103–113.
[50] D. Gumy, A.G. Rincon, R. Hajdu, C. Pulgarin, Solar Energy 80 (2006) 1376–1381.
[51] P.M. Murno, G.N. Flatatau, L.R. Clement, M.L. Gauthier, Appl. Environ. Microbiol. 61 (1995) 1853.
[52] M. Child, P. Strike, R. Pickup, C. Edwards, FEMS Microbiol. Lett. 213 (2002) 81.
[53] A.G. Rincon, C. Pulgarin, Appl. Catal. B 44 (2003) 263.
[54] J. Feng, X. Hu, P.L. Yue, H.Y. Zhu, G.Q. Lu, Chem. Eng. Sci. 58 (2003) 679–685.
[55] A.G. Rincon, C. Pulgarin, Sol. Energy 77 (2004) 635.
[56] Section: Surfaces and Microanalysis. DIN 39 and DIN nm, Norms of the National Physics Laboratory, Teddington, UK, 2003, p. 816.